Determination of the Distance Dependence and Experimental Effects for Modified SERS Substrates Based on Self-Assembled Monolayers Formed Using Alkanethiols

B. J. Kennedy, S. Spaeth,† M. Dickey, and K. T. Carron*

Chemistry Department, University of Wyoming, Laramie, Wyoming 82071

Received: November 17, 1998; In Final Form: February 16, 1999

Modified SERS (surface-enhanced Raman scattering) substrates are based on self-assembled monolayers (SAMs) formed from compounds such as alkanethiols. Chain lengths ranging from ethanethiol to octadecanethiol were used to investigate properties of modified SERS substrates. These properties include determining the magnitude of the SERS electromagnetic enhancement, developing a sensitivity factor for detecting aromatic compounds, and evaluating SERS substrates for performance characteristics such as stability and solvent effects. A SERS electromagnetic enhancement was determined to be 2.1×10^3 for detecting aromatic compounds. The effects of experimental conditions on the SERS detection process were addressed. SERS sensitivity was shown to be highly dependent upon a correlation between the SERS interfacial distance dependence and a hydrophobic effect exhibited by the alkyl chain of the thiol. The distance dependence was more significant than the hydrophobic effect for detecting aromatic compounds. For comparison to the electromagnetic enhancement, a SERS sensitivity factor was determined for detecting benzene in water and in organic solvents. Experimental stability issues, such as solvent and laser exposure, were shown to affect the sensitivity of modified SERS substrates. 1-Propanethiol exhibited the strongest sensitivity and stability under all solvent and experimental conditions.

Introduction

One method for preparing modified SERS (surface-enhanced Raman scattering) substrates is to apply analyte specific coatings based on self-assembled monolayers (SAMs) onto a roughened SERS metal surface. These types of substrates demonstrate sensitive and selective detection for a variety of analytes including organics[1] and metal ions[2] and as coatings for optical fiber sensors.[3] SERS sensors have been implemented for detection capabilities in gas chromatography (GC),[4] liquid chromatography (LC), and flow-injection analysis (FIA),[5,6] and for drug analysis using thin-layer chromatography.[7] Other applications of SERS chemical sensors involve developments for increased sensitivity, selectivity, and biocompatibility.[8−13]

In this work, SERS substrates are analyzed as analytical sensors for their ability to detect aromatic compounds. Several approaches are used to measure the distance dependence and magnitude of the SERS electromagnetic (EM) enhancement, and to investigate the stability and sensitivity of alkanethiol-modified SERS substrates. The method used in this work involves self-assembled monolayers (SAMs) of straight-chain alkanethiols on acid-roughened Ag foil substrates. The thiol of a straight-chain alkanethiol will bond to Ag surfaces and form well-ordered monolayers. The monolayer can act as a spacer to determine both the distance dependence of SERS and by extrapolation, the EM enhancement. Implementing these modified SERS substrates for in situ techniques requires the investigation of coating sensitivity and stability while maintaining the requirement for the SERS interfacial distance dependence.

SERS can be explained by two distinct enhancement mechanisms: chemical enhancement[14] and electromagnetic enhancement (EM).[15] The chemical enhancement results when a molecule coordinates with a metal surface and forms charge transfer states with energy levels in the metal. This leads to a charge transfer transition in the visible wavelength region and a surface localized resonance Raman enhancement. A key to the difference between chemical and EM enhancements is that the chemical enhancement is strictly limited to molecules in direct contact with the surface.

The EM portion of SERS occurs most notably with properly roughened silver, copper, and gold surfaces that have roughness features smaller than the wavelength of light.[16,17] The EM enhancement observed with these noble metals is attributed to their electron configuration. Each metal has an electron configuration of $d^{10}s^1$ in the zero oxidation state. The d^{10} configuration causes the s^1 electron to be shielded from the nucleus, allowing the s^1 electron to have free electron character. When visible light is incident on the metal surface, the free electron condition leads to a dielectric constant of the metal composed of a large negative real component and a small imaginary component. The magnitude and sign of the dielectric constant determine whether SERS occurs.

The simplest expression that describes the EM enhancement is the electric field at a small spherical particle,

$$E_{\text{local}} = \left(\frac{1}{\epsilon(\omega) + 2}\right) E_0 \qquad (1)$$

where E_{local} is the local electric field due to the polarization of the particle, ω is the frequency of the incident radiation, $\epsilon(\omega)$ is the overall dielectric constant of the metal at the frequency ω, and E_0 is the electric field of the incident radiation. According to this equation, the local electric field will approach infinity when the dielectric constant approaches -2. For silver $\epsilon(\omega)_{\text{real}} = -2$ in the near-UV.[18] The small imaginary part of the dielectric constant keeps the EM enhancement finite.

* To whom correspondence should be addressed.

† 1996 Research Experience for Undergraduates Program at UW Chemistry Department, from Fort Lewis College, Durango, CO.

10.1021/jp984454i CCC: $18.00
Published on Web 04/15/1999

The EM enhancement occurs since the local field described by eq 1 oscillates at the frequency of the incident radiation as a dipolar optical radiation source and can be scattered by molecules near the surface. Furthermore, the dipolar radiation scattered by the molecules near the surface is capable of coupling to the metal particle and enhancing the scattered light. These two sources of EM enhancement are multiplicative and couple to give a total enhancement proportional to the local fields,

$$EF = E(\omega_0)^2_{\text{local}} E(\omega_{\text{Raman}})^2_{\text{local}} \quad (2)$$

where ω_0 is the laser frequency and ω_{Raman} is $(\omega_0 - \Delta\omega_{\text{Raman shift}})$. The Raman effect can be described as the dipolar field of the particle inducing a radiating dipole in the molecule. This is similar to a London dispersion type interaction and has a distance dependence of $1/r$.[6] An analogous distance dependence is found for the dipole induced in the particle by the dipolar field of the scattering molecule. Therefore, the overall distance dependence of the EM enhancement is $1/r$.[12] Taking into account the increasing surface area as one considers shells of molecules around the sphere leads to a r^2 increase in molecules, and thus an overall $1/r^{10}$ distance dependence for the EM enhancement of SERS.

The $1/r^{10}$ dependence is purely theoretical and in practice does not represent the true distance dependence. This is due to variations in the particle shapes and sizes which leads to deviations from eq 1. Interparticle interactions also lead to coupled fields that tend to average the single-particle description of SERS and lead to deviations from the $1/r^{10}$ distance dependence. On the other hand, it is important that the EM enhancement and its distance dependence be accurately measured to provide a quantitative guide for the growing number of SERS analytical applications.

The affinity process for selective analyte adsorption to SERS coatings can be described analogously to retention mechanisms[19] used for describing bonded phase materials in reversed-phase liquid chromatography (RPLC), although controversy remains in both cases. Column coatings provide affinity sites for analyte retention where separations are performed using appropriate mobile phases. Retention of a given analyte to both column coatings and SERS coatings increases with increasing alkyl chain length. In both cases a "critical chain length" can be found. With chromatography, retention has been shown to increase from C_6 to C_{10} and level off for longer chains.[20] *n*-Alkanethiols have also been used to enhance selectivity for HPLC electrochemical detection of hydrophobic compounds over other electroactive species. This study looked at chain lengths from C_8 to C_{18}, where a critical chain length of C_{10} provided optimum current permeability for maximum selectivity.[21]

This illustrates, analogous to the SERS effect, that electron transport (for SERS, electric fields) diminishes with increasing distance from the substrate. Based on theoretical and experimental results, interfacial SERS electromagnetic enhancements decrease exponentially with increasing chain length for *n*-alkyl groups chemically bound to the roughened Ag surface.[22,23] Interfacial enhancement also occurs for molecules coadsorbed to surface coatings. Molecules closer to the surface experience a greater local electric field enhancement than do those that are further away from the surface. SERS coating selection is therefore empirically based on the decrease in SERS with increasing chain length (i.e., distance from the surface). Because of this, the sensitivity of 1-propanethiol (**C3**) is markedly improved over other similar but longer chain thiols where the molecules cannot closely approach the surface roughness features.

A primary advantage to using modified SERS substrates over normal Raman spectroscopy and other SERS methods[24] is that the surface sensitivity can be replenished by flowing streams. This allows for continuous detection capabilities. A substantial concern is the issue of surface stability during continuous analysis, such as in GC or LC. The gas phase sensitivity is the highest where competitive interactions between the mobile phase (helium) and the SERS coatings are minimal.[4] Therefore, the SERS detection process is maximized or ideal. Under aqueous conditions the sensitivity was reduced.[5] Sensitivity is further reduced by the presence of organic solvents such as methanol. In this work, solvent effects are addressed in more detail to illustrate how they influence SERS sensitivity, and monolayer conformational changes and stability. Although SERS substrates demonstrate stability in air and water over periods of months,[25] a substantial concern is the issue of surface stability during continuous analysis, such as in GC or LC. A further understanding of these issues is pertinent to the development of SERS coatings and sensors that provide ideal sensitivity and stability.

Experimental Section

All chemicals were purchased from Aldrich (except tetradecanethiol, synthesized by a published route)[26] and used without further purification: silver foil (0.1 mm, 99.9%), absolute methanol, absolute ethanol, 1-propanethiol (99%), 1-pentanethiol (98%), 1-octanethiol (97+%), decanethiol (98%), dodecanethiol (98%), hexadecanethiol (92%), and octadecanethiol (98%). For brevity, the thiols are referred to as **C3**, **C5**, **C8**, **C10**, **C12**, **C14**, **C16**, and **C18**, respectively. In the distance dependence study the benzene and *tert*-butylbenzene aqueous solutions were saturated. The saturated benzene solution was measured using GC-MS to be 8.6×10^{-3} M, and the saturated *tert*-butylbenzene solution was measured using GC-MS to be 1.6×10^{-4} M. To analyze solvent effects, solutions were prepared to be 8.6×10^{-3} M benzene in water (Millipore, 18 MΩ) or methanol:water ($MeOH:H_2O$) solutions. Data treatment involved reference subtraction of coating signals using respective water or methanol:water solutions, from which benzene intensities could be obtained.

The SERS methodology for preparing acid etched substrates was initially described by Miller *et al.*[27] and has since been elaborated on for applications to Ag.[1−7] Nitric acid etched substrates are used because they are applicable to analytical applications, are easily prepared, and have been shown to be the most sensitive of the water stable surfaces.[8] In this work, the process first involved cleaning the surface with a methanol rinse followed by a water rinse. Clean foils are acid etched in 30% nitric acid for approximately 1 min with vigorous stirring. Following the etch process, surfaces are vigorously rinsed in water and also with ethanol before submerging in the thiol solutions. The coatings used in this study (**C3**−**C18**) were applied by soaking the foil in a 1 mM ethanolic solution of the different thiols for at least 24 h. Before use the foils were gently washed with ethanol (to remove coadsorbed thiols) and allowed to air-dry. A reproducible surface preparation process is essential to compare different thiols. This was most accurately performed using a batch process where a large substrate was prepared before being divided into sections and coating with respective thiols. This quantitative etching process is the best method for comparing surfaces without introducing variations due to changing etch conditions (time, temperature, acidity).

In all the experiments described comparable results have been obtained for several replicate trials but are reported for an individual trial, unless otherwise noted. By comparable, we refer to the reproducibility of similar trends but must also mention that identical curve shapes are not readily reproducible. This is most applicable to the stability study (Figure 5). When comparing different monolayers or solvent systems, the reported results represent those from a batch surface preparation. For example, when comparing the sensitivity of thiols **C3**−**C18**, a large foil was prepared. It was cut into smaller pieces that were soaked in respective thiol solutions. These were assumed to be similar at the spectroscopic level allowing comparisons to be made between different coatings. To illustrate the necessity of this technique a simple experiment was performed. First, 10 individual surfaces were prepared as described above and soaked in 1mM **C3**. This yielded a root mean deviation (RMD) of 21% for evaluation of the (C−S) peak areas at 715 cm^{-1}. Using the batch preparation method, a large foil was etched and cut into 10 pieces before soaking in a 1 mM **C3** solution. This approach yielded a RMD of 6%. Therefore, batch surface preparations provide improved reproducibility between surfaces prepared in this manner. The 6% RMD is being assumed to represent fluctuation in surface roughness features that are present on an individual surface.

A conventional optics-based Raman system optimized for 647 nm excitation and 30 mW has been described previously. S/N was optimized with a combination of 647 nm interference filters (holographic notch filter (Kaiser Optics) and a holographic edge filter (POC)). Surfaces were rigidly fixed in a custom aluminum holder that fit squarely in a 1 cm^2 quartz cuvette. The cuvette was capped during the Raman measurement to prevent the evaporation of the organics from the aqueous solutions. This gave 45° surface alignment with respect to the quartz windows and allowed complete solution interaction with the SERS substrate. To prevent direct reflection of the laser beam into the collection optics the laser focus entered ca. 95° from the quartz interface allowing for a collection angle at ca. 85° from the SERS substrate. Signal optimizing was performed in a focus mode to eliminate Schlerian effects as the solution refractive index changed. The spectra in the distance dependence study were smoothed using a 9-point Savitsky-Golay smoothing routine in Lab Calc and were also baseline corrected. Additional spectral analysis is described with corresponding figures. Data analysis was performed using GRAMS/32 spectroscopy software. Unless otherwise noted, spectral results are normalized for equivalent exposure times. These were 240 s for the sensitivity experiments and 300 s for the stability analysis.

Results and Discussion

SERS Distance Dependence. The purpose in doing this study was to provide an accurate determination of the absolute SERS enhancement on an analytically practical silver substrate and to determine the SERS distance dependence from the silver surface. The integrity of these results is derived from careful control over the SERS substrate fabrication, proof that the coatings did not have pinholes or defects, and an examination of the intercalation of probe molecules (benzene and *tert*-butylbenzene) into the coatings. The presence of significant pinholes was ruled out using pyridine as a surface sensitive probe. If there are defects in the coatings, the distances between the organic molecules and the silver surfaces will not be consistent. Pyridine was chosen as the surface probe since it has distinct spectral differences between its hydrogen bonded form in an aqueous matrix compared to its chemisorbed form on a silver surface. Pyridine hydrogen bonded with water shows a ring-breathing mode at 1003 cm^{-1} in comparison to the ring-breathing mode at 1008 cm^{-1} when pyridine is coordinated with silver.[28] If pinhole defects are present in the film then pyridine modes at 1008 cm^{-1} would be evident in the spectra of the modified SERS substrates. The spectral analysis of an octanethiol-modified SERS surface in the presence of a 0.5 M pyridine solution indicates that silver sites are not accessible for chemisorption of pyridine. This simple test of coating quality indicates that these SAMs will not allow the distance dependence probes (benzene or *tert*-butylbenzene) to adsorb to the silver. The less ordered monolayer systems formed from shorter chain thiols were assumed to allow intercalation to occur, as discussed below with Figure 4. For this reason the distance dependence is determined using thiols **C8**−**C18**. Representative spectra and relevant SAM formation concepts for alkanethiols adsorbed on Ag are readily available.[29,30]

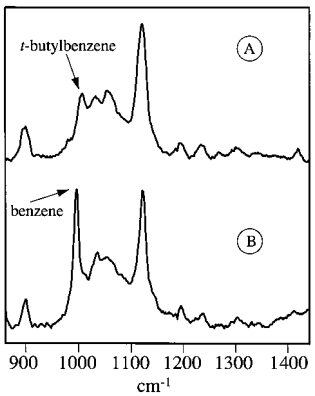

Figure 1. SERS spectra of *tert*-butylbenzene (A) and benzene (B) adsorbed to an octanethiol-modified SERS substrate before reference subtraction. Additional examples of representative SERS spectra and subtraction results can be found in ref 1.

The above experiments indicate that silver sites are not available for coordination when the coating is a high-integrity self-assembled monolayer. A second series of experiments was performed to examine the potential for intercalation of single ring species into the monolayer. Such intercalation is analytically advantageous since it would lead to stronger SERS signals and a larger dynamic range through loading of the coating on the silver surface. The intercalation probes chosen for this study are benzene and *tert*-butylbenzene, spectra are shown in Figure 1 using an octanethiol coating. An assumption is that *tert*-butylbenzene will not be able to penetrate into the self-assembled monolayers. In Figure 2, the SERS intensities of benzene and *tert*-butylbenzene adsorbed to the alkanethiol SAMs were measured and normalized to take into account the different Raman cross sections of the two molecules. The distance of the molecule from the surface, *r*, was varied by using alkanethiols with different chain lengths.[31] As the thicknesses of the alkanethiol SAMs were increased, it was observed that the Raman peak intensity (*I*) of benzene and *tert*-butylbenzene adsorbed to the SAMs decreased (Figure 2). Theory predicts that a plot of log(*I*) versus log((*a*+*r*)/*a*) should have a slope of −10

$$I = \left(\frac{a + r}{a}\right)^{-10} \tag{3}$$

where *a* is the radius of curvature of the roughness feature on the silver surface.[32]

Assuming that *tert*-butylbenzene is sterically hindered from intercalating into the SAMs, eq 3 predicts a slope of −10 for

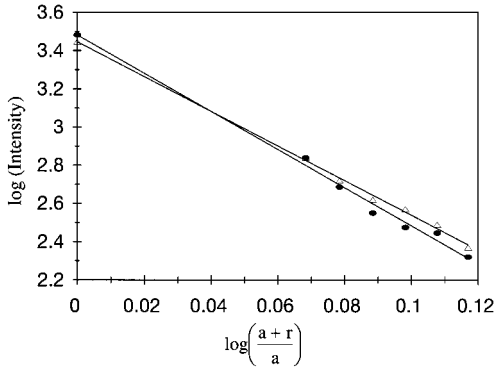

Figure 2. Plot of SERS intensity (*I*) for benzene (●) and *tert*-butylbenzene (□) as a function of alkanethiol chain length. From right to left, the points correspond to **C18**, **C16**, **C14**, **C12**, **C10**, **C8**, and extrapolation to zero (i.e., no coating), respectively. The variable *a* is the radius of curvature for the SERS enhancing sphere and *r* represents alkanethiol chain length, both in nm. SERS spectral intensity for benzene is decreasing with increasing carbon number. Experimental parameters given in the text.

the *tert*-butylbenzene plot in Figure 2. The radius of curvature values were found by varying the *a* factor to produce a slope of −10. The calculated radius of curvature was found to be 9.3 nm which is in the range of values measured with atomic force microscopy (AFM) for nitric acid roughened silver surfaces. The slope of −9.1 for the benzene plot in Figure 2 indicates that benzene does intercalate into the alkanethiol surface coating. This also allows us to assume that the monolayers systems are of high integrity.

Calculation of the Electromagnetic Enhancement. The planar area of the SERS substrate excited by the laser was calculated to be 4.1×10^{-8} m^2 using the beam waist and height of the laser beam. Double potential step chronocoulometry has shown that the true surface area of a roughened substrate is approximately 7 times greater than the planar surface area.[33] This makes the actual SERS substrate surface area excited by the laser approximately 2.9×10^{-7} m^2. Assuming that one monolayer of benzene is adsorbed to the SAM, the number of benzene molecules excited by the laser in the SERS measurements can be calculated using 3.0 D for the radius of benzene in a liquid at 20 °C.[34] The cross-sectional area of benzene is calculated to be 2.8×10^{-19} m^2 per benzene molecule. Therefore, the number of benzene molecules excited by the laser with SERS is calculated to be 1.03×10^{12} molecules [$(2.9 \times 10^{-7})/(2.8 \times 10^{-19})$].

For the theoretical enhancement of benzene at the silver surface (for a chain length of zero), the number of photons per benzene molecule can be determined from the intercept of the benzene plot in Figure 2. The *y*-intercept for benzene corresponds to 2800 photons. Using this basis the number of photons per benzene molecule is calculated to be 2.7×10^{-9}. This value, when coupled with the photons/benzene molecule observed by normal Raman spectroscopy, allows the determination of the electromagnetic enhancement at the surface.

The intensity of a Raman spectrum of bulk benzene was measured to be 5400 photons using the same laser intensity and acquisition time as the SERS measurements. The volume of benzene molecules excited was calculated to be 6.2×10^{-13} m^3 using the beam waist and height of the laser beam, and the slit width of the spectrograph. This volume of benzene is equivalent to 4.1×10^{15} benzene molecules. Therefore, for normal Raman there were 1.3×10^{-12} photons per benzene molecule.

The SERS EM enhancement is calculated by dividing the number of photons per benzene molecule detected with SERS by the number detected with normal Raman [$(2.7 \times 10^{-9})/(1.3 \times 10^{-12})$]. Therefore, for the roughened silver substrates used in this work the SERS EM enhancement is determined to be 2.1×10^3. As discussed below, this value compares reasonably well with what other researchers have found, although the methods and results of previous distance dependence studies vary greatly.[35−38]

The SERS EM enhancement has been experimentally determined to be between 10^2 and 10^7.[35,36] Assuming that the chemical enhancement is 10^2, Murray's EM would be 10^3−10^4. Also, it was believed that the complex morphology of the Ag films could cause variations in the enhancements of individual PNBA molecules depending on if they were adsorbed to the top or sides of a Ag protrusion, by a factor of 10^4. Bohn and Walls did not actually calculate the EM enhancement of SERS, but they did find an exponential decrease in the signal intensity as the spacer thickness was increased.[37] Schatz and Zeman's calculation of the EM enhancement was determined to be 10^5 for Ag at 647.1 nm.[38] A discrepancy between our experimental value and this theoretical value can be accounted for by assuming optimal size and shape. A more appropriate range of particle shapes for acid-etched substrates could be from 1 to 100 nm. By changing the value for particle shapes (*a* in eq 3) it is possible for the EM enhancement to range from 5400 for an *a* value of 1 nm, to 1770 for an *a* value of 100 nm. However, changing the *a* value introduces a deviation from the theory presented above for eq 3.

Solvent Effects on SERS Sensitivity. Previous efforts show that maximum SERS enhancements for benzene detection are obtained using a 1-propanethiol (**C3**) SERS substrate.[39] Detection limits for benzene were near 5 ppm. Although short chains maximize coupling with interfacial SERS enhancements, their affinity for analytes (increasing for more hydrophobic compounds (e.g., ethylbenzene) and stability were expected to be lower than that for longer chain thiols. Several presumptions were made to develop this assumption. First, longer chain thiols yield more ordered monolayer systems and are thus more stable, due to greater van der Waals interactions between adjacent alkyl chains.[31] Second, with increasing chain length, the hydrophobic effect of the longer chains should enhance the sensitivity. The relevance of these issues to in situ SERS detection is associated with the effects of solvents on the SERS/analyte interaction process and the anticipation that longer chain thiols will retain analyte selectivity under harsh solvent conditions. To study this we have chosen the following alkanethiols: **C3**, **C5**, **C8**, **C12**, and **C18**.

As a coating for modified SERS substrates, alkanethiols produce monolayer structures that provide low surface energy SAMs. These SAMs create an affinity for hydrophobic compounds, i.e., aromatics, which are known to experience a high solvation energy in aqueous media. Comparable to the SERS distance dependence discussed above, results are shown for absolute benzene intensities as a function of chain length and increasing methanol concentration (Figure 3). This includes short-chain thiols such as **C3**. As shown in Figure 4, at 100% H_2O, this distance dependence drops off roughly exponentially with distance from the underlying SERS roughness features. Based on greater hydrophobic effects for longer alkyl chains, it was expected that with increasing chain length the analytes would be preconcentrated close to the surface. An observed disadvantage is that the longer chains inversely serve to separate the analytes from the large local electric fields at the surface. Of significance under all solvent conditions is that **C3** displays marked enhancement over the other thiols. **C3** is also affected

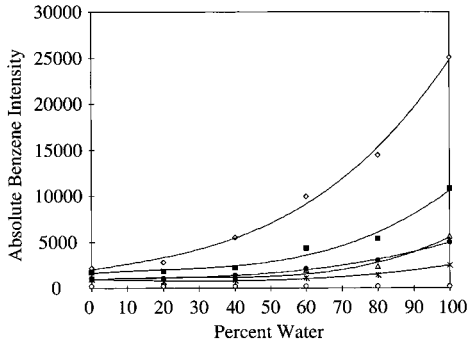

Figure 3. Plot of SERS intensity (*I*) for benzene as a function of both increasing alkanethiol chain length and increasing methanol concentration, for respective alkanethiols: **C3** (◇), **C5** (■), **C8** (△), **C12** (●), **C18** (*), no surface (○). Exposure times were 240 s each with 647 nm excitation and 30 mW. The benzene concentration was 8.6×10^{-3} M for each sample. This illustrates the SERS distance dependence and the effects of organic solvents on analyte affinity to modified SERS substrates.

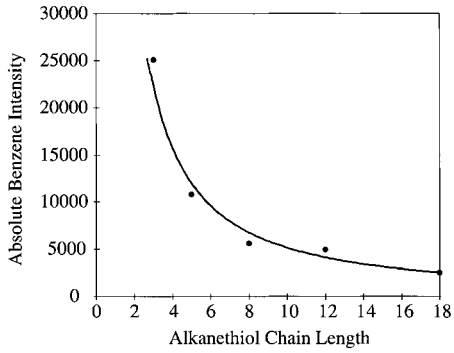

Figure 4. Plot of SERS intensity (*I*) for 8.6×10^{-3} M benzene in water as a function of increasing alkanethiol chain length, again illustrating the SERS interfacial distance dependence. Conditions identical to those in Figure 3.

more by methanol, as noted by its larger slope in comparison to the other thiols, an issue returned to below. This implies that the SERS/analyte interaction process is hydrophobic in nature and that affinity, thus sensitivity, decreases with analyte miscibility in organic solutions.

A sensitivity factor was developed based on detection of benzene in water using normal Raman (i.e., no SERS substrate). Under identical conditions used in developing Figure 3, an intensity count of 250 ADU (DL $\cong$ 350 ppm, $\sigma_{noise} = 28$) was obtained for 8.6×10^{-3} M benzene in water. In Figure 3, for **C3**, the intensity of the benzene signal is 24 992 ADU. Comparing the SERS result to the Raman result correlates to a sensitivity factor of 100. This rapidly decreases with both increasing chain length and methanol concentrations. The *sensitivity* factor does not account for the total number of benzene molecules in solution being interrogated by the laser versus the number at the SERS interface as would be necessary for comparison to the SERS *enhancement* factor. In the distance dependence study, the SERS EM enhancement factor was calculated to be over 2000 for the adsorption of benzene directly on a SERS substrate, assuming there to be no alkanethiol surface moieties. By extrapolating for **C3** in Figure 2, using the same method as above for the theoretical adsorption of benzene on silver, the EM should be well over 1000. The factor of 10 difference between the theoretical EM and the observed enhancement can be attributed to a greatly reduced availability of adsorption sites that are occupied by the alkanethiol assemblies. Without the alkane groups, the high surface energy silver substrate would prevent the necessary SERS adsorption process.

For **C3**, spectral evidence does not conclusively indicate that benzene is adsorbed directly to the SERS surface. This would be a significant observation indicating the ability for analytes to fully intercalate into the monolayer structure. Evidence for benzene intercalating into the monolayer can be drawn upon from the results in Figure 4. First, benzene intensities at 100% H_2O increase rapidly when the chain length decreases from **C5** to **C3**. The marked sensitivity increase for **C3** can possibly be attributed to benzene coming in close contact or possibly adsorbing (physisorption) to the silver substrate. Spectral results from this work do not support the physisorption of benzene onto silver but only provide information related to benzene adsorbing to the thiol coatings. The a_{1g} ring-breathing mode at 992 cm^{-1}, and the e_{2u} C−H deformation at 849 cm^{-1} are not affected by adsorption, but the appearance of the normally Raman-forbidden a_{2u} C−H deformation at 703 cm^{-1} would clearly indicate the adsorption of benzene on silver.[40] The absence of this occurrence indicates that analytes do not fully intercalate into alkanethiol monolayer assemblies. Evidence for less than single monolayer coverage of benzene on all thiols is also found by the lack of the e_{2g} mode at 614 cm^{-1}. The e_{2g} mode arises when benzene is able to orient parallel to the Ag surface. With adequate monolayer coverage, this parallel orientation is expected to not be possible.

On the basis of contact angle measurements (**C3** 94°, **C5** 104°, **C8** 109°, **C12** 112°, **C18** 115°) for alkanethiols on smooth Ag,[41,42] we expect benzene to have lower surface affinity for short chain length monolayers. Roughened substrates demonstrate very low wettability (θ > 145° for all thiols on acid-roughened silver in this study) and do not provide quantitative information for elucidating solvent effects on SERS sensitivity.[43] Solution compositions appear to have a greater influence on selectivity in SERS adsorption processes than do the modified SERS coatings. For SERS, the interaction occurs through competitive hydrophobic interactions of analytes between the solution and the coating/solution interface. The purpose in illustrating these aspects involving modified SERS substrates is that their use for real-time analysis is limited to specific molecular arrangements chemically bound to noble metals. These points conclude that, of primary importance in SERS methodologies, the requirement is to couple with the large local electric fields residing close to the roughened metal surface, more so than incorporating long-chain alkanethiols for enhanced selectivity. Since **C3** provides significant enhancements for detecting aromatic compounds under all solvent conditions and for stability issues discussed below, we confine further investigations of solvent effects to **C3** only.

Experimental and Solvent Effects on SERS Coating Stability. A primary method for extracting analyte information for analytes adsorbed onto a SERS coating is to perform a reference subtraction of the coating signal. However, coating signals can fluctuate either due to overall coating degradation with associated peak shifts or through increasing or decreasing trans/gauche modes. The latter point suggests that the coating is undergoing conformational changes with decreased ordering. Besides reducing the SERS affinity process the presence of solvents also induces ordering/disordering of the hydrophobic alkyl chains. This may be dependent on solvent penetration between alkyl chains. Spectrally, these factors contribute to reduce the effectiveness of the reference subtraction for obtaining analyte information. As a result, subtraction residuals are

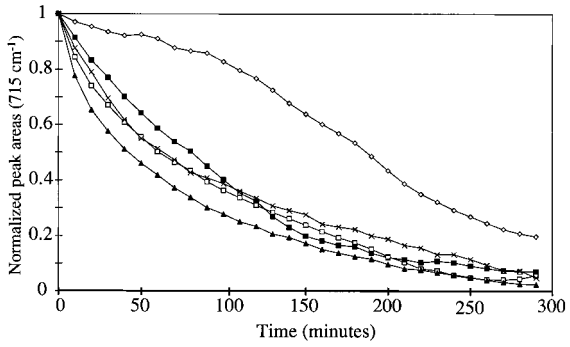

Figure 5. Plot of peak area (ν(C−S) trans vibrational mode at 715 cm^{-1})) versus exposure time. The peak areas are normalized to the area at time zero for respective thiols: **C3** (◇), **C5** (□), **C8** (▲), **C12** (*), and **C18** (■). Exposure times were 300 s with 647 nm excitation and 30 mW with the SERS substrate in air. This illustrates clearly that 1-propanethiol forms the most stable monolayer system for modified SERS substrates. The other systems (**C5**−**C18**) each demonstrate similar stability in comparison to **C3**.

often more intense than analyte signals thereby reducing the ability to obtain good sensitivity.

Coating degradation in air occurs through thermal processes upon laser exposure to the monolayers (Figure 5). An anticipated result was that coating stability would increase with increasing chain length. Maximized van der Waals interactions between longer chain alkanethiols provide improved monolayer ordering and assumed better stability. However, **C3** clearly provides the greatest stability over the other thiols **C5**−**C18**. The significance of this observation, and the fact that **C3** provides the greatest sensitivity, is that 1-propanethiol is clearly the best coating for detecting aromatic compounds using SERS techniques. A problem that must still be surmounted is the issue of stability. As mentioned previously, the changing spectral conditions lead to poor reference subtractions and therefore reduced sensitivity.

The observed behavior of **C3** as a SERS coating is quite different from published results for short-chain thiols.[30,44] Figure 5 evaluates the trans ν(C−S)frequency for the laser-induced degradation of self-assembled monolayers in air. A batch surface preparation method was used for comparing surfaces with different coatings. With this method each figure represents results from a new surface and, although the trends are reproducible, obtaining identical line shapes was more difficult.

A possible explanation for the stability of the short-chain thiol is that monolayer formation rates decrease with increasing chain length.[45] Although the adsorption rates for longer chain thiols onto Au exceeds that for short-chain thiols, stable monolayer formation through interchain interactions is more rapid for shorter chain thiols. Another possibility is that **C3**, a short-chain thiol, can more effectively cover the underlying surface roughness features, allowing the formation monolayers that are more stable. Spectrally it provides very intense signals in comparison to the other thiols. This may also infer the marked sensitivity increase for **C3** over **C5**−**C18**, as discussed above. However, the continuous degradation of monolayers during a real-time analysis reduces our ability to monitor the affects of solvents on the alkyl chain assemblies. Using SERS, these changing monolayer conformations can be evaluated under various solvent conditions while considering the overlapping affects of experimental monolayer degradation.

Since **C3** clearly exhibits the greatest sensitivity under various solvent conditions and the most ideal stability as a SERS sensor coating, it has become the focus of several other investigations related to solvent and experimental effects. Although monolayers formed on Au and Ag are typically interpreted using IR techniques and can be evaluated in situ with PM-IRRAS,[46] the real time, in situ analysis for solvent effects on the entire monolayer assembly can be evaluated using SERS. The PM-IRRAS results indicate monolayer conformational changes upon solvent exposure. Similarly, we observe varying conformational changes as a function of varying solvent exposure. For example, in air, the monolayer systems degrade rapidly during continuous laser exposure (647 nm, 30 mW). The systems also degrade faster while using higher laser powers (100 mW) or while using lower wavelength sources (514 nm, 30 mW). Both of these effects are observed due to the increased power density at the sample.

The **C3** coated substrates were also subjected to continuous solvent exposure using the 647 nm source, 30 mW. Conformation characteristics of alkanethiols have been previously discussed in the literature.[47,48] The SERS substrates used in this study were initially most stable in methanol, followed by those in water, and were the least stable in air. After ca. 90 min of continuous laser exposure all substrates displayed substantial degradation regardless of the sampling medium. This suggests that the laser induced thermal load to the sample was initially being quenched by the solvent medium. However, once degradation was initiated, it continued throughout the 3 h exposure time. An additional observation was that the ν(C−S) trans and gauche modes were not degrading at identical rates. Therefore, the coatings were undergoing conformational changes while degradation occurs. It is important to note that, although the samples do degrade during long exposures (>60 min), all samples are adequately stable for the short exposure times required for typical analytical methods.

Conclusions

The electromagnetic enhancement (EM) of SERS for Ag using SAMs of straight-chain alkanethiols was measured. By increasing the number of carbons making up the alkanethiols, we were able to increase the distance that adsorbed benzene and *tert*-butylbenzene were from the Ag. This spacer experiment allowed us to measure the decrease in the Raman signal from the benzene and *tert*-butylbenzene as the chain length increased. The *y*-intercept of the graph relating SERS intensity to separation distance was used to determine the signal expected for a SAM chain length of zero. Comparing these signals to the Raman signals from bulk benzene and *tert*-butylbenzene, we were able to measure the EM of Ag SERS which was found to be 2.1×10^3. This value is within the range of measurements obtained by other researchers. We were also able show that surface quality was high which would keep any chemical enhancement from occurring, and therefore, the measurement was strictly due to the EM of SERS.

The most distinct observation from this work is that, during continuous sampling, self-assembled monolayer systems are of varying stability and conformation regardless of solvent or ambient conditions or excitation sources and powers. Unstable systems limit the further development of SERS detection systems. Short-chain thiols, **C3** in particular, proved most useful in that they enable analytes to couple with the large local electric fields and they also provide excellent stability. This process occurs to a limiting value. Ethanethiol and methanethiol both have very poor sensitivity and stability, partially attributed to a combination of reduced aromatic affinity and that they are highly reactive with the Ag substrate. This later point suggests that propanethiol may also be highly reactive with Ag, thus explaining its marked sensitivity and stability over longer chain thiols. In conclusion, it is obvious that stability gains would be

benficial. A possibility for meeting this requirement would be to develop polymerizable monolayers[49,50,51] that also maintain the SERS distance dependence requirements.

Acknowledgment. The authors acknowledge the AFOSR Grant no. 93-NA-187. Dr. Carron would like to acknowledge partial support from NSF Grant number EPS-9550477.

References and Notes

(1) Carron, K.; Peitersen, L.; Lewis, M. *Environ. Sci. Technol.* **1992**, *26*, 1950−1954.
(2) Crane, L. G.; Wang, D.; Sears, L. M.; Heyns, B.; Carron, K. *Anal. Chem.* **1995**, *67*, 360−364.
(3) Mullen, K. I.; Carron, K. T. *Anal. Chem.* **1990**, *63*, 2196−2199.
(4) Carron, K. T.; Kennedy, B. J. *Anal. Chem.* **1995**, *67*, 3353−3356.
(5) Kennedy, B. J.; Milofsky, R.; Carron, K. T. *Anal. Chem.* **1997**, *69*, 4708−4715.
(6) Weissenbacher, N.; Lendl, B.; Frank, J.; Wanzenbock, H. D.; Mizaikoff, B.; Kellner, R. *J. Mol. Struct.* **1997**, *410*−*411*, 539−542.
(7) Horvath, E.; Mink, J.; Kristof, J. *Mikrochim. Acta, Suppl.* **1997**, *14*, 745−746.
(8) Norrod, K. L.; Sudnik, L. M.; Rousell, D.; Rowlen, K. L. *Appl. Spectrosc.* **1997**, *51*, 994−1001.
(9) Mullen, K.; Carron, K. T. *Anal. Chem.* **1994**, *66*, 478−483.
(10) Heyns, J. B.; Sears, L. M.; Corcoran, R. C.; Carron, K. T. *Anal. Chem.* **1994**, *66*, 1572−1574.
(11) Maeda, Y.; Yamamoto, H.; Kitano, H. *J. Phys. Chem.* **1995**, *99*, 4837−4841.
(12) Wachter, E. A.; Storey, J. M. E.; Sharp, S. L.; Carron, K T.; Jiang, Y. *Appl. Spectrosc.* **1995**, *49*, 193−199.
(13) Storey, J. M. E.; Barber, T. E.; Wachter, E. A.; Carron, K T.; Jiang, Y. *Spectroscopy* **1995**, *10*, 21−25.
(14) Seki, H. *J. Chem. Phys.* **1982**, *9*, 4412−4418.
(15) Mullen, K. I.; Wang, D.; Crane, L. G.; Carron, K. T. *Spectroscopy* **1992**, *7*, 24−35.
(16) Wokaun, A. *Solid State Phys.* **1984**, *46*, 223−294.
(17) Vo-Dinh, T.; Bello, J. M. *Appl. Spectrosc.* **1990**, *44*, 63−69.
(18) In *Surface Enhanced Raman Scattering*; Chang, R. K., Furtak, T. E., Eds.; Plenum Press: New York, 1982.
(19) Dorsey, J. G.; Cooper, W. T. *Anal. Chem.* **1994**, *66*, 857A−867A.
(20) Berendsen, G. E.; De Galan, L. *J. Chromatogr.* **1980**, *196*, 21−37.
(21) Liu, Z.; Li, J.; Dong, S.; Wang, E. *Anal. Chem.* **1996**, *68*, 2432−2436.
(22) Kerkers, M.; Wang, D.; Chew, H. *Appl. Opt.* **1980**, *19*, 4159−4174.
(23) Gersten, J.; Nitzan, A. *J. Chem. Phys.* **1980**, *73*, 3023−3037.
(24) (a) Pothier, N. J.; Force, R. K. *Anal. Chem.* **1990**, *62*, 678−680. (b) Ni, F.; Thomas, L.; Cotton, T. M. *Anal. Chem.* **1989**, *61*, 888−894. (c) Soper, S. A.; Ratzlaff, K. L.; Kuwana, T. *Anal. Chem.* **1990**, *62*, 1438−1444. (d) Cabalín, L. M.; Rupérez, A.; Laserna, J. J. *Anal. Chim. Acta* **1996**, *318*, 203−210.
(25) Deschaines, T.; Carron, K. T. *Appl. Spectrosc.* **1997**, *51*, 1355−1359.
(26) Urquhart, G. G.; Gates, J. W. Jr.; Connor, R. *Organic Synthesis Collective Volume 3*; Horning, E. C., Ed.; Wiley: New York, 1955; pp 363−365.
(27) Miller, S. K.; Baiker, A.; Meier, M.; Wokaun, A. *J. Chem. Soc., Faraday Trans. 1* **1984**, *80*, 1305−1312.
(28) Fleischmann, M.; Hill, I. R. *Surface Enhanced Raman Scattering*; Chang, R. K, Furtak, T. E., Eds.; Plenum Press: New York, 1982; p 277.
(29) Joo, T. H.; Kim, M. S. *J. Phys. Chem.* **1986**, *90*, 5816−5819.
(30) (a) Bryant, M. A.; Pemberton, J. E. *J. Am. Chem. Soc.* **1991**, *113*, 3629−3637. (b) Bryant, M. A.; Pemberton, J. E. *J. Am. Chem. Soc.* **1991**, *113*, 8284−8293.
(31) Porter, M. D.; Bright, T. B.; Allara, D. L.; Chidsey, C. E. D. *J. Am. Chem. Soc.* **1987**, *109*, 3559−3568.
(32) Murray, C. A. *Surface Enhanced Raman Scattering*; Chang, R. K., Furtak, T. E., Eds.; Plenum Press: New York, 1982; p 208.
(33) Lakovits, J., Ph.D. Thesis, Northwestern University, 1981.
(34) Israelachvili, J. N., *Intermolecular and Surface Forces*; Academic Press: San Diego, CA, 1992; p 111.
(35) Kovacs, G. J.; Loutfy, R. O.; Vincett, P. S. *Langmuir* **1986**, *2*, 689−694.
(36) Murray, C. A.; Allara, D. L. *J. Chem. Phys.* **1982**, *76*, 1290−1303.
(37) Walls, D. J.; Bohn, P. W. *J. Phys. Chem.* **1989**, *93*, 2976−2982.
(38) Zeman, E. J.; Schatz, G. C. *J. Phys. Chem.* **1987**, *91*, 634−643.
(39) Jiang, Y. Ph.D. Thesis, University of Wyoming, 1995.
(40) (a) Perry, S. S.; Hatch, S. R.; Campion, A. *J. Chem. Phys.* **1996**, *104*, 6856−6859. (b) Moskovits, M.; DiLella, D. P. In *Surface Enhanced Raman Scattering*; Chang, R. K., Furtak, T. E., Eds.; Plenum Press: New York, 1982; pp 243−274.
(41) Laibinis, P. E.; Whitesides, G. M.; Allara, D. L.; Tao, Y.; Parikah, A. N.; Nuzzo, R. G. *J. Am. Chem. Soc.* **1991**, *113*, 7152−7167.
(42) Walczak, M. M.; Chung, C.; Stole, S. M.; Widrig, C. A.; Porter, M. D. *J. Am. Chem. Soc.* **1991**, *113*, 2370−2378.
(43) Drelich, J.; Miller, J. D.; Good, R. J. *J. Colloid Interface Sci.* **1996**, *179*, 37−50.
(44) Camillone, N.; Chidsey, C. E. D.; Liu, G.; Scoles, G. *J. Chem. Phys.* **1993**, *98*, 3503−3511.
(45) Karpovich, D. S.; Blanchard, G. J. *Langmuir* **1994**, *10*, 3315−3322.
(46) Anderson, M. R.; Evaniak, M. N.; Zhang, M. *Langmuir* **1996**, *12*, 2327−2331.
(47) Poirier, G. E.; Tarlov, M. J.; Rushmeier, H. E. *Langmuir* **1994**, *10*, 3383−3386.
(48) Camillone, N.; Chidsey, C. E. D.; Liu, G.; Putvinski, T. M.; Scoles, G. *J. Chem. Phys.* **1991**, *94*, 8493−8502.
(49) Mowery, M. D.; Evans, C. E. *Tetrahedron Lett.* **1997**, *38*, 11−14.
(50) Kim, T.; Chan, K. C.; Crooks, R. M. *J. Am. Chem. Soc.* **1997**, *119*, 189−193.
(51) Willicut, R. J.; McCarley, R. L. *Adv. Mater.* **1995**, *7*, 759−762.